Check for updates

Water Science & Technology

IWA PUBLISHING

© 2021 The Authors

Water Science & Technology Vol 84 No 12, 3907 doi: 10.2166/wst.2021.483

Effect of nozzle geometry on the dynamics and mixing of self-similar turbulent jets

Pourya Nejatipour and Babak Khorsandi*

Department of Civil and Environmental Engineering, Amirkabir University of Technology (Tehran Polytechnic), Tehran, Iran
*Corresponding author. E-mail: b.khorsandi@aut.ac.ir

BK, 0000-0003-4088-9740

ABSTRACT

The effect of nozzle geometry on the dynamics and mixing of turbulent jets is experimentally investigated. The jets with a Reynolds number of 13,000 were issued from four different pipes with circular, elliptical, square and triangular cross sections. The velocity field was measured in the self-similar region of the jets using an acoustic Doppler velocimeter. Statistical parameters, such as the mean velocities, velocity variances, spreading rates, mass flow rates, and entrainment rates are presented. The results show that despite having approximately similar decay rates for the mean centerline velocities, the radial profiles of the axial mean velocity varied in jets with different nozzle cross sections and were widest for elliptical jets and narrowest for the triangular ones. On the other hand, velocity variances were greatest for the triangular jet when compared to the jets released from cross sections of other geometries. Furthermore, the spreading rate, mass flow rate, and entrainment rate were highest for the elliptical jet, and lowest for the triangular jet. From this it can be inferred that the elliptical jet has the highest mixing and dilution. The results of this study could help to improve the initial mixing of pollutants by optimizing the initial conditions.

Key words: acoustic doppler velocimeter, dynamic, mixing, nozzle geometry, turbulent jets

HIGHLIGHTS

- Radial velocity profiles were widest for the elliptical jets and narrowest for the triangular jets.
- In the self-similar region, velocity variances were greatest for the triangular jets.
- Elliptical jets have the highest entrainment and mixing.

INTRODUCTION

Many industrial activities result in accidental and planned releases of pollutants into rivers, lakes, seas and oceans. Such releases can adversely affect the aquatic life as well as the ecosystem. The effluents from coastal industries that are released into the ambient environment must be mixed and diluted within a short time and distance to lower their adverse impacts. Therefore, the most important process for reducing these deleterious effects in the hydrosphere is the dilution of pollutants.

Pollutants are usually introduced into the water-receiving environment in the form of turbulent jets that have high mixing capabilities. Turbulent jets entrain the clean ambient fluid as they develop and as a result their mass flow rate increases and their concentration deceases with the downstream distance. Turbulent round jets have received considerable research attention because of their fundamental and practical importance. The study of turbulent round jets dates back to the work of Trüpel (1914) and Schlichting (1933), but since then many interesting aspects of their dynamics have been discussed in studies such as Wygnanski & Fiedler (1969), Hussein *et al.* (1994), Panchapakesan & Lumley (1993), Darisse *et al.* (2015) and Moeini *et al.* (2021).

One of the important jet parameters that can affect its dynamics and mixing is the initial conditions of the jet releases. Initial conditions here refer to initial turbulence level, Reynolds number, nozzle type (exit velocity profiles), nozzle geometry, and aspect ratio (AR) of non-circular nozzles. Nozzle types can be classified as contoured or smooth contracting nozzles, orifice plates, and long pipes. Long pipes are usually used in practice to release the pollutants into the environment. Various researchers have investigated the effect of initial conditions of the mixing and turbulent characteristics of jets (Goldschmidt & Bradshaw 1981; Ho & Gutmark 1987; Quinn 1991; Lee & Baek 1994; Abdel-Rahman *et al.* 1996; Mi *et al.* 2001, 2007; Mi &

This is an Open Access article distributed under the terms of the Creative Commons Attribution Licence (CC BY-NC-ND 4.0), which permits copying and redistribution for non-commercial purposes with no derivatives, provided the original work is properly cited (http://creativecommons.org/licenses/by-nc-nd/4.0/).

Downloaded from http://iwaponline.com/wst/article-pdf/84/12/3907/980074/wst084123907.pdf
by guest

Nathan 2010; Xu *et al.* 2013a, 2013b). In particular, it has been shown that the nozzle type and Reynolds number influence the flow downstream from the point of release (Mi *et al.* 2001, 2009; Xu & Antonia 2002).

The effect of initial conditions of circular jets have been studied. The statistics of top-hat and pipe jets were shown to be similar in the self-similar region (Ferdman *et al.* 2000; Antonia & Zhao 2001; Xu & Antonia 2002). The mixing performance of a round jet issuing from three nozzle types (i.e. pipe, orifice and smooth contraction) has also been investigated. The results revealed that the orifice plate nozzle provided the highest rate of mixing and the pipe jet had the least mixing with the ambient fluid (Mi *et al.* 2001). Furthermore, the orifice jets had higher rate of decay and entrainment compared to the top-hat jets in the near-field region (Quinn *et al.* 2013).

Non-circular jets have been experimentally and numerically studied by various researchers because of their potential to enhance mixing between jets and the ambient fluid (Ho & Gutmark 1987; Hussain & Husain 1989; Quinn 1989, 2005; Grinstein *et al.* 1995; Miller *et al.* 1995; Mi *et al.* 2000). Considerable research efforts have also been made to understand the effects of nozzle geometry on mixing performance and turbulence characteristics of turbulent jets in the near-field (Hussain & Husain 1989; Mi *et al.* 2001; Quinn 2005; Mi & Nathan 2010; Azad *et al.* 2012; Hashiehbaf & Romano 2013; Quinn *et al.* 2013; Xu *et al.* 2013a, 2013b; Aleyasin *et al.* 2017). In general, it has been found that the loss of axisymmetry of the orifice nozzle configuration increases the decay rate of mean and RMS velocities in the near-field, from which higher entrainment into the jet may be concluded (Mi *et al.* 2001). Furthermore, it has been shown that the jets issuing from elliptic nozzles and nozzles with corners have better mixing performance when compared to circular jets in the near- and intermediate-fields (Ho & Gutmark 1987; Hussain & Husain 1989; Quinn 2005; Aleyasin *et al.* 2017).

Despite numerous studies on the effect of nozzle geometry on the statistics and mixing characteristics of jets in the developing region and near-fields, to the authors' knowledge, no thorough study has been conducted in the self-similar region (intermediate- to far-field) of pipe jets. It has also been claimed that the statistics in the self-similar region may depend on the initial conditions (George & Arndt 1989). Furthermore, many of the past studies only focused on the mean velocity and turbulence intensities along the centerline (Mi *et al.* 2000; Mi & Nathan 2010; Azad *et al.* 2012; Quinn *et al.* 2013). In the present experimental study, the dynamics and mixing in the self-similar region of turbulent jets, released from pipes with different cross sections, are investigated. The pipes had cross sections of circle, square, equilateral triangle, and ellipse. The instantaneous velocities were measured using an acoustic Doppler velocimeter, and statistics including the mean velocities, velocity variances, spreading rates, mass flow rates, and entrainment rates are presented.

EXPERIMENTAL SETUP

In this section, the experimental setup, including the jet apparatus, flume, and acoustic Doppler velocimeter (ADV) are discussed. Experiments were conducted in a $1 \times 1.7 \times 0.54$ m upstream concrete basin connected to a 6-m long flume filled with water (Figure 1).

Jet nozzles consist of pipes with four circular, square, elliptical and (equilateral) triangular cross sections which were made using a 3D printer. All jet nozzles had identical cross section area with equivalent diameter (D_e) of 1 cm. D_e is defined as the diameter of a circle with the same area as a non-circular area. The aspect ratio for the elliptical jet was 1.5. The jets were discharged in the mid-depth of the (upstream basin of the) flume. To achieve a fully developed outlet jet, the nozzle was extended for 20 cm (equivalent to $20D_e$) after the bend. The jets were fed by a constant head tank located at a height of 2.5 m above the ground. The Reynolds number of the jets $\mathrm{Re} = U_j D_e/\nu$ (where, U_j is the outlet velocity of the jet nozzle, and ν is the kinematic viscosity of water) was set to 13,000, corresponding to an outlet (average) velocity of approximately 1.30 m/s. As the jets were fed from the flume water, the temperature of the jet and the fluid surrounding the jet were similar.

The velocity field was measured using a Nortek 10-MHz ADVLab acoustic Doppler velocimeter (ADV). Measurements were made downstream of the jets from $x/D_e = 15$–95 (where, x is the downstream distance from the jet nozzle). The sampling frequency of the ADV was set to 25 Hz (maximum). To ensure statistics convergence, measurements were conducted for 30 min. As depicted in Figure 2, the x-axis of the probe was aligned with the axis of the jet and its y and z axes were aligned with the horizontal and vertical radial directions of the jet, respectively. To increase the signal-to-noise ratio, talcum powder was added to water (Khorsandi *et al.* 2012; Moeini *et al.* 2020). The velocity range of ADV was set to ± 10 cm/s, ± 30 cm/s and ± 100 cm/s to span the entire range of the velocities measured at each point. The sampling volume height was set to its maximum value of 9 mm, which increased the signal-to-noise ratio and consequently reduced the Doppler noise

Downloaded from http://iwaponline.com/wst/article-pdf/84/12/3907/980074/wst084123907.pdf
by guest

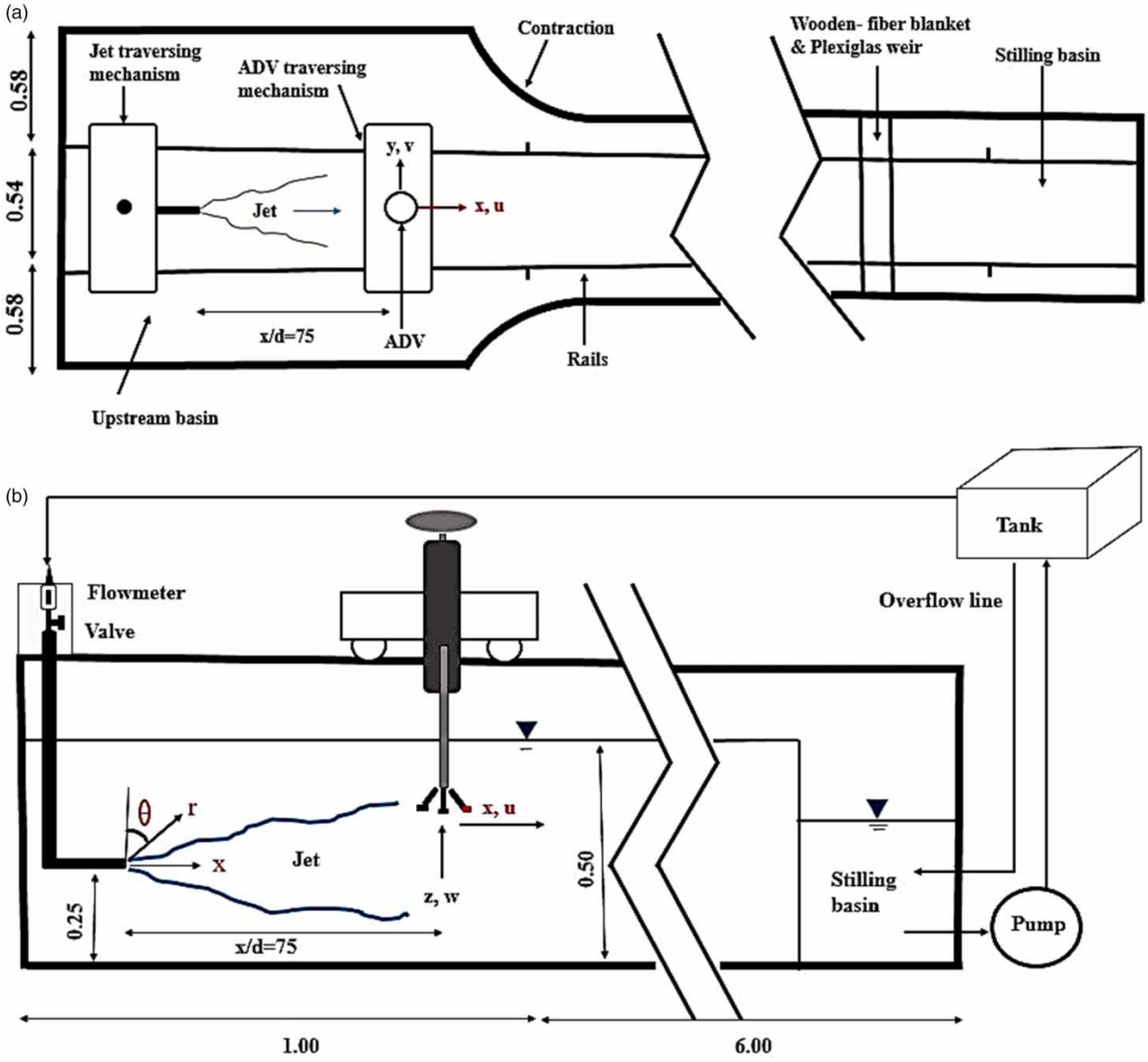


Figure 1 | The experimental setup including the flume, jet and ADV. (a) Top view), (b) side view.

(Kazemi *et al.* 2021). The ADV data was post-processed using the WinADV software, which is based on the noise-reduction method of Nikora & Goring (1998) modified by Wahl (2003).

RESULTS

In this section, the statistics, including the mean axial velocities, velocity variances spreading rates, mass flow rates, and entrainment rates of jets issuing from four different nozzles with circular, elliptical, square and triangular cross sections, are presented. The results are compared with those of Mi & Nathan (2010), Panchapakesan & Lumley (1993), Ricou & Spalding (1961), Hussein *et al.* (1994) and Khorsandi *et al.* (2013).

The downstream evolution of the inverse of the normalized mean axial centerline velocity of the jet (U_j/U_{cl}, where U_{cl} is mean axial centerline velocity) is shown in Figure 3. It can be seen that the inverse of mean velocities varies linearly with the downstream distance (or the mean velocities decay approximately as x^{-1}), in the self-similar region. The linear fit can be described by $<U_{cl}>/U_j = B/[(x–x_0)/D_e]$, where x_0 is the virtual origin of the jet and B is the decay constant. The estimates

Downloaded from http://iwaponline.com/wst/article-pdf/84/12/3907/980074/wst084123907.pdf
by guest

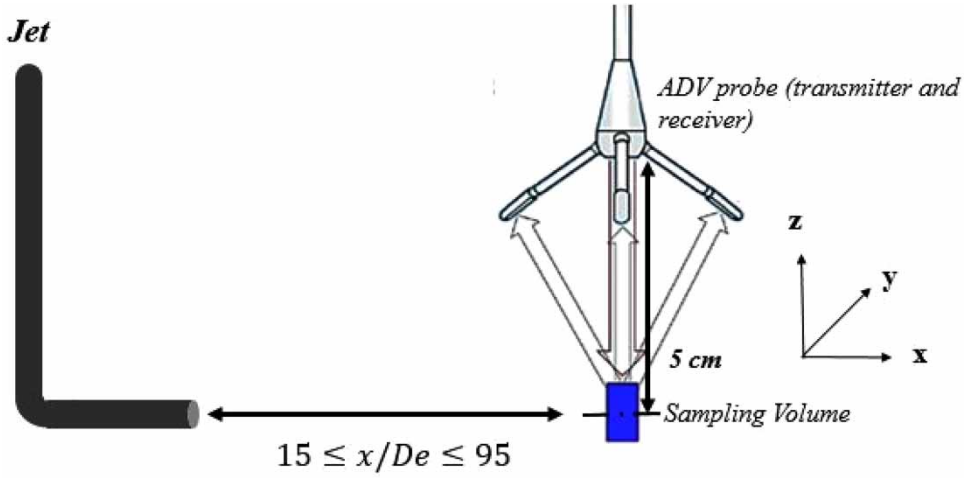


Figure 2 | The schematic of the circular jet and ADV.

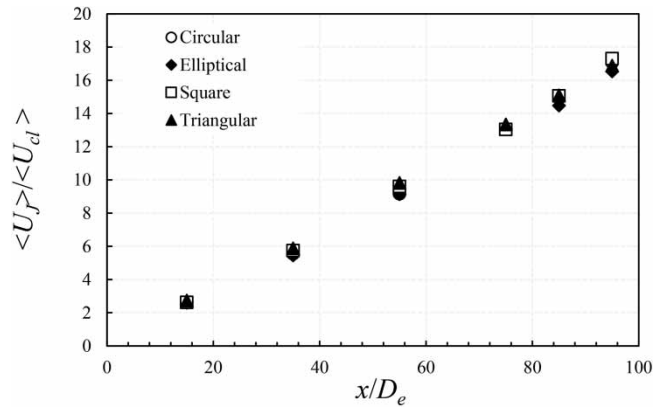


Figure 3 | Downstream evolution of the centerline axial mean velocity of four turbulent jets at Re = 13,000.

of B obtained for nozzles with different cross-sections are compared in Table 1. As can be observed, the decay constants are similar for jets with different cross sections in the self-similar region. Furthermore, the decay constants are lower than those of orifice plate jets measured in the near-field by Mi & Nathan (2010). The difference may probably be due to the different nozzle type, measurement region, and measurement technique.

The radial profiles of the axial mean velocity measured for four turbulent jets at $x/D_e = 75$ are presented in Figure 4. (As the profiles were symmetric, only half of the profiles are presented.) The profiles are compared with the circular jet profile of Panchapakesan & Lumley (1993). It can be seen that the profiles of jets with different cross sections agree well around the centerline, however, the difference between the profiles increases in the range $0.1 \leq r/x \leq 0.17$. The mean velocity profile of the triangular jet falls slightly under the data of the other nozzles. On the other hand, the profile of the elliptical jet is a bit higher and wider than those of the other jets. The difference between the profile of circular jet and that of Panchapakesan & Lumley (1993) may be due to the different nozzle type. In addition, the lower velocities at the edge of the jet are probably due to the return flow, which is common in enclosures, and affect smaller velocities more significantly (Hussain & Husain 1989; Kazemi *et al.* 2021).

The radial profiles of the axial mean velocity measured for jets with different cross sections at three downstream distances ($x/D_e = 35$, 55 and 75), are presented in Figure 5. It can be seen that the profiles are self-similar for each cross section in the range of measurement. Nevertheless, the initial conditions of the jets affect the profiles. The elliptical jets show a higher degree of self-similarity compared to the other profiles, especially the triangular jets.

The jet spreads linearly in the self-similar region and its spreading rate is defined as $S \equiv \mathrm{d}r_{1/2}/\mathrm{d}x$, where, $r_{1/2}$ is the jet's half-width (Pope 2000). The half-width (a measure of jet's width) is the radial position where the velocity reaches half of its

Downloaded from http://iwaponline.com/wst/article-pdf/84/12/3907/980074/wst084123907.pdf
by guest

Table 1 | The velocity decay constant (B), spreading rate (S) and entrainment rate (E) for four turbulent jets

Study	Nozzle geometry	Nozzle type	Measurement technique	AR	Range of x/D_e	Re	x_o/D_e	B[a]	S	E
Present	Circular	Pipe	ADV	1	15–95	13,000	2.76	5.72	0.098	0.27
Present	Elliptical	Pipe	ADV	1.5	15–95	13,000	2.05	5.69	0.104	0.30
Present	Square	Pipe	ADV	1	15–95	13,000	2.13	5.70	0.098	0.28
Present	Equilateral triangular	Pipe	ADV	1	15–95	13,000	2.56	5.66	0.094	0.24
Khorsandi *et al.* (2013)	Circular	Pipe	ADV	1	35–75	10,600	4	5.66	0.099	0.30
Ricou & Spalding (1961)	Circular	Orifice plate	Micromanometer	1	0–400	25,000	–	–	–	0.32
Panchapakesan & Lumley (1993)	Circular	Contoured	Hot-wire anemometry	1	30–160	11,000	0	6.06	0.096	–
Mi & Nathan (2010)	Circular	Orifice plate	Hot-wire anemometry	1	11–40	15,000	0.6	6.41	–	–
Mi & Nathan (2010)	Elliptical	Orifice plate	Hot-wire anemometry	2	8–40	15,000	−0.8	6.17	–	–
Mi & Nathan (2010)	Square	Orifice plate	Hot-wire anemometry	1	8–40	15,000	0.5	6.36	–	–
Mi & Nathan (2010)	Equilateral triangular	Orifice plate	Hot-wire anemometry	1	5–40	15,000	−1.0	6.13	–	–

[a]The value of B was calculated for the range of $15 \leq x/D_e \leq 75$ due to increased uncertainty at $x/D_e > 75$.

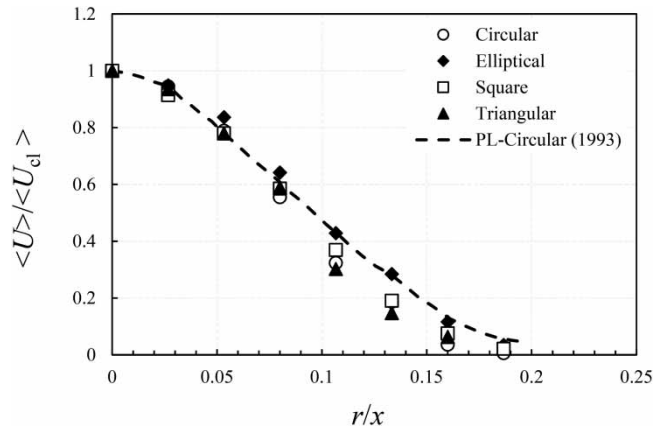


Figure 4 | Radial profile of the mean axial velocity of four turbulent jets ($x/D_e = 75$). The broken line represent the data of Panchapakesan & Lumley (1993).

maximum value. The spreading rate of the jets with different cross sections were calculated from the radial profiles of the axial mean velocities measured at $x/D_e = 35$, 55 and 75. The spreading rates are presented in Table 1. It can be observed that the triangular and elliptical jets have the minimum and maximum spreading rates, respectively. This is in agreement with the narrower profile of the triangular jet and the wider profile of the elliptical jet seen in Figure 4. The spreading rates of circular and square jets are similar.

The mass flow rate of jets increases as they develop downstream due to the entrainment of the ambient fluid into the jets. By integrating the area under the radial profiles of the mean axial velocity (Figure 5), the mass flow rate values were calculated at different downstream locations and are depicted in Figure 6. The mass flow rates are normalized by the mass flow rate at the nozzle exit, m_0. The jet entrainment rates (*i.e.*, dm/dx, where m is the mass flow rate) were obtained from the downstream

Downloaded from http://iwaponline.com/wst/article-pdf/84/12/3907/980074/wst084123907.pdf
by guest

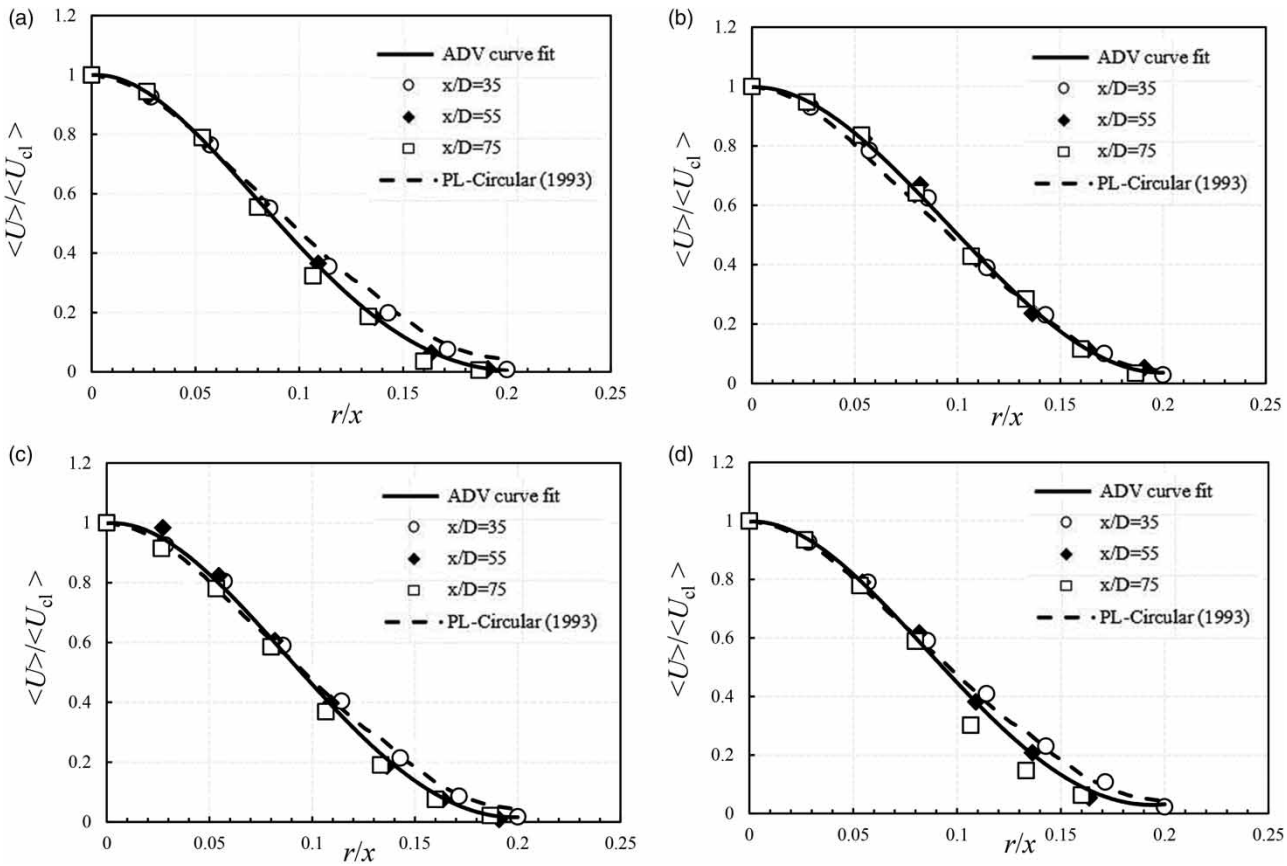


Figure 5 | Radial profile of the mean axial velocity of four turbulent jets at $x/D_e = 35$, 55 and 75. (a) Circular; (b) elliptical; (c) square; (d) triangular; the solid line represents ADV curve fit. The broken line represents the data of Panchapakesan & Lumley (1993).

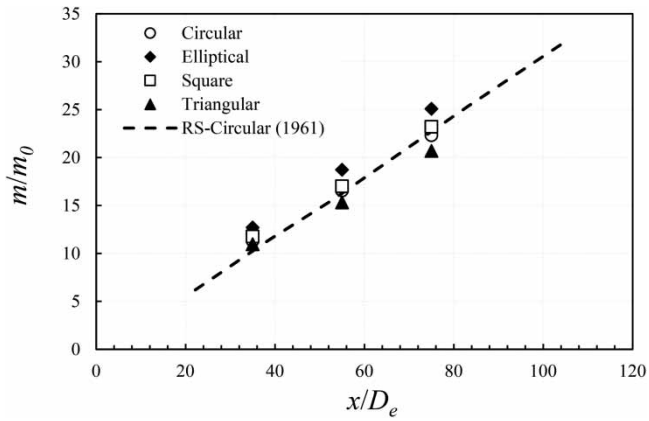


Figure 6 | The downstream evolution of the mass flow rate of four turbulent jets. The broken line represents the data of Ricou & Spalding (1961).

evolution of mass flow rates and are presented in Table 1. The results show that the mass flow rate and the entrainment rate are highest for the elliptical jet and lowest for the triangular jet. This is consistent with the measurements of the spreading rates, indicating that the elliptical jets spread relatively faster than the other jets. From the higher mass flow rate and entrainment rate of the elliptical jet, it can be inferred that the mixing and dilution is probably higher in elliptical jets.

The centerline axial and radial velocity variances of the jet (normalized by the square of the centerline mean axial velocities) are shown in Figure 7. The normalized velocity variances become self-similar at around $x/D_e > 75$. The

Downloaded from http://iwaponline.com/wst/article-pdf/84/12/3907/980074/wst084123907.pdf
by guest

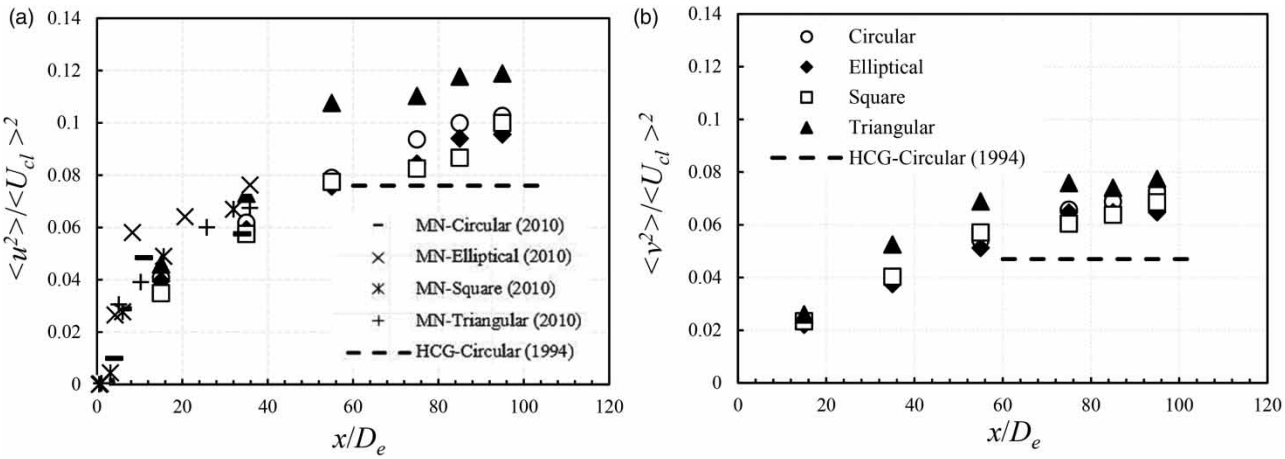


Figure 7 | Downstream evolution of the velocity variances at the centerline of four turbulent jets. (a) axial velocity variances; (b) radial velocity variances; The data of Hussein *et al.* (1994) (HCG) and Mi & Nathan (2010) (MN) are also included for comparison. Other symbols are the same as in Figure 7(b).

normalized velocity variances are approximately constant in the self-similar region as both the RMS velocities ($<u_i^2>^{1/2}$) and the mean axial velocities decay as x^{-1}. It can also be seen that the normalized velocity variances of the triangular jet are higher than those of the other jets. The elliptical and square jets have the lowest velocity variances in the self-similar region. It is worth noting that as the mean axial velocities of jets released from different nozzles along the centerline are similar (see Figure 4), the differences observed here between the data of different nozzles are mainly due to the variations in the velocity variances. In addition, the axial velocity variances of Mi & Nathan (2010) measured in the near-field are also plotted in Figure 7(a). (Note that the radial velocity variances were not presented in Mi & Nathan (2010)). As observed, these data have different trend (e.g., elliptical jets have the highest velocity variances) probably because of different initial conditions and the spatial range of measurement.

The radial profiles of axial and radial velocity variances, normalized by the square of the centerline mean velocity, at $x/D_e = 75$, are plotted in Figure 8. The figure shows that the velocity variances of the triangular jet are noticeably higher than those of the other jets (similar to what was observed for the centerline velocity variances in Figure 7). On the other hand, the velocity variances of circular, square and elliptical jets are similar. The differences between the velocity variances of jets with different cross sections decrease when moving toward the outer regions of the jets as the velocity variances decrease. Note that the velocity variances are relatively higher than those of circular jet of Hussein *et al.* (1994). This

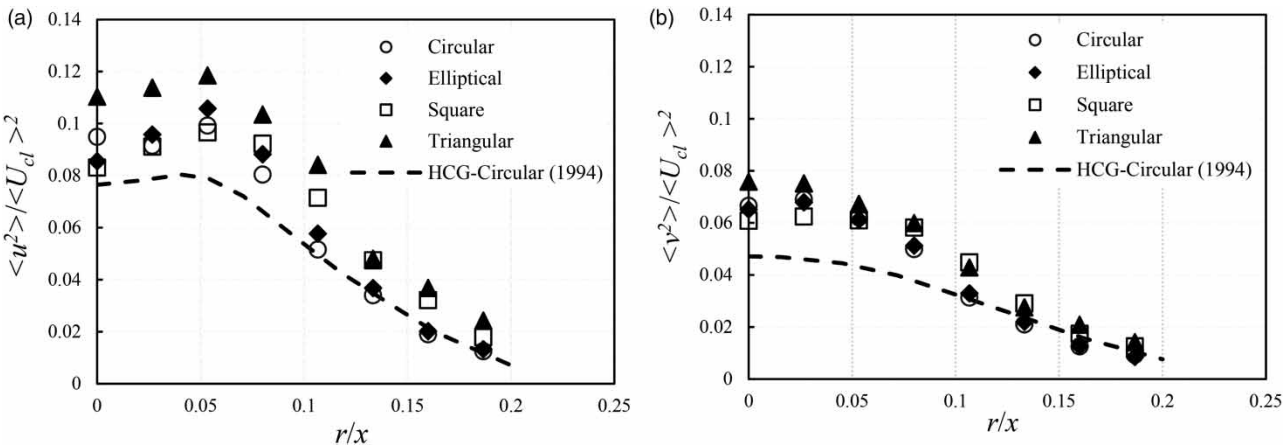


Figure 8 | Profiles of velocity variances of four turbulent jets at Re = 13,000 and $x/D_e = 75$. (a) Axial velocity variances; (b) radial velocity variances. The broken line represents the data of Hussein *et al.* (1994).

Downloaded from http://iwaponline.com/wst/article-pdf/84/12/3907/980074/wst084123907.pdf
by guest

difference may be attributed to different initial conditions and the fact that ADVs overestimate the velocity variances due to the higher noise in turbulent measurements.

CONCLUSION

The effect of nozzle geometry on the dynamics and mixing of turbulent jets issued into a quiescent background was experimentally investigated. The statistical parameters such as the axial mean velocities, velocity variances, spreading rates, mass flow rates, and entrainment rates of jets released from pipes with circular, elliptical, square and (equilateral) triangular cross sections, and with the same equivalent diameters, were reported. The results showed that the shape of the nozzle cross section, can affect the jet statistics in the self-similar region. Although the mean axial velocities along the centerlines of jets with different cross sections were similar, however, the radial profile of the mean axial velocities were relatively wider in the elliptical jet and narrower in the triangular jet. The spreading rate, mass flow rate, and entrainment rate of the elliptical jet were higher than those of the other jets. As a result it is expected that elliptical jets have higher rate of dilution and mixing. The velocity variances in both axial and radial directions were higher in triangular jets than those of the other jets that had similar velocity variances.

FUNDING

This research did not receive any specific grant from funding agencies in the public, commercial or not-for-profit sectors.

AVAILABILITY OF DATA AND MATERIAL

The dataset on which this paper is based is too large to be retained or publicly archived with available resources. Documentation and methods used to support this study are available from the corresponding author upon reasonable request.

DATA AVAILABILITY STATEMENT

All relevant data are included in the paper or its Supplementary Information.

REFERENCES

Abdel-Rahman, A. A., Al-Fahed, S. F. & Chakroun, W. 1996 The near-field characteristics of circular jets at low Reynolds numbers. *Mechanics Research Communications* **23** (3), 313–324. https://doi.org/10.1016/0093-6413(96)00028-6.

Aleyasin, S. S., Tachie, M. F. & Koupriyanov, M. 2017 PIV measurements in the near and intermediate field regions of jets issuing from eight different nozzle geometries. *Flow, Turbulence and Combustion* **99** (2), 329–351. https://doi.org/10.1007/s10494-017-9820-3.

Antonia, R. A. & Zhao, Q. 2001 Effect of initial conditions on a circular jet. *Experiments in Fluids* **31** (3), 319–323. https://doi.org/10.1007/s003480100289.

Azad, M., Quinn, W. R. & Groulx, D. 2012 Mixing in turbulent free jets issuing from isosceles triangular orifices with different apex angles. *Experimental Thermal and Fluid Science* **39**, 237–251. https://doi.org/10.1016/j.expthermflusci.2012.01.028.

Darisse, A., Lemay, J. & Benaissa, A. 2015 Budgets of turbulent kinetic energy, Reynolds stresses, variance of temperature fluctuations and turbulent heat fluxes in a round jet. *Journal of Fluid Mechanics* **774**, 95. https://doi.org/10.1017/jfm.2015.245.

Ferdman, E., Otugen, M. V. & Kim, S. 2000 Effect of initial velocity profile on the development of round jets. *Journal of Propulsion and Power* **16** (4), 676–686. https://doi.org/10.2514/2.5627.

George, W. K. & Arndt, R. 1989 *The Self-Preservation of Turbulent Flows and its Relation to Initial Conditions and Coherent Structures*. Advances in Turbulence. Hemisphere, New York, USA, p. 3973. https://doi.org/10.1007/BF00189015.

Goldschmidt, V. W. & Bradshaw, P. 1981 Effects of nozzle exit turbulence on the spreading/or widening/rate of plane free jets. In: *American Society of Mechanical Engineers and American Society of Civil Engineers, Joint Applied Mechanics, Fluids Engineering, and Bioengineering Conference*. University of Colorado, Boulder, CO, USA.

Grinstein, F. F., Gutmark, E. & Parr, T. 1995 Near field dynamics of subsonic free square jets. A computational and experimental study. *Physics of Fluids* **7** (6), 1483–1497. American Institute of Physics. https://doi.org/10.1063/1.868534.

Hashiehbaf, A. & Romano, G. P. 2013 Particle image velocimetry investigation on mixing enhancement of non-circular sharp edge nozzles. *International Journal of Heat and Fluid Flow* **44**, 208–221. https://doi.org/10.1016/j.ijheatfluidflow.2013.05.017.

Ho, C.-M. & Gutmark, E. 1987 Vortex induction and mass entrainment in a small-aspect-ratio elliptic jet. *Journal of Fluid Mechanics* **179**, 383–405. https://doi.org/10.1017/S0022112087001587.

Hussain, F. & Husain, H. S. 1989 Elliptic jets. Part 1. Characteristics of unexcited and excited jets. *Journal of Fluid Mechanics* **208**, 257–320. https://doi.org/10.1017/S0022112089002843.

Hussein, H. J., Capp, S. P. & George, W. K. 1994 Velocity measurements in a high-Reynolds-number, momentum-conserving, axisymmetric, turbulent jet. *Journal of Fluid Mechanics* **258**, 31–75. https://doi.org/10.1017/S002211209400323X.

Downloaded from http://iwaponline.com/wst/article-pdf/84/12/3907/980074/wst084123907.pdf
by guest

Kazemi, M., Khorsandi, B. & Mydlarski, L. 2021 Effect of acoustic Doppler velocimeter sampling volume size on measurements of turbulence. *Journal of Atmospheric and Oceanic Technology* **38**, 259–268. https://doi.org/10.1175/JTECH-D-20-0174.1.

Khorsandi, B., Mydlarski, L. & Gaskin, S. 2012 Noise in turbulence measurements using acoustic Doppler velocimetry. *Journal of Hydraulic Engineering* **138** (10), 829–838. https://doi.org/10.1061/(ASCE)HY.1943-7900.0000589.

Khorsandi, B., Gaskin, S. & Mydlarski, L. 2013 Effect of background turbulence on an axisymmetric turbulent jet. *Journal of Fluid Mechanics* **736**, 250–286. https://doi.org/10.1017/jfm.2013.465.

Lee, S.-J. & Baek, S.-J. 1994 The effect of aspect ratio on the near-field turbulent structure of elliptic jets. *Flow Measurement and Instrumentation* **5** (3), 170–180. https://doi.org/10.1016/0955-5986(94)90016-7.

Mi, J. & Nathan, G. J. 2010 Statistical properties of turbulent free jets issuing from nine differently-shaped nozzles. *Flow, Turbulence and Combustion* **84** (4), 583–606. https://doi.org/10.1007/s10494-009-9240-0.

Mi, J., Nathan, G. J. & Luxton, R. E. 2000 Centreline mixing characteristics of jets from nine differently shaped nozzles. *Experiments in Fluids* **28** (1), 93–94. https://doi.org/10.1007/s003480050012.

Mi, J., Nathan, G. J. & Nobes, D. S. 2001 Mixing characteristics of axisymmetric free jets from a contoured nozzle, an orifice plate and a pipe. *Journal of Fluids Engineering* **123** (4), 878–883. https://doi.org/10.1115/1.1412460.

Mi, J. B., Kalt, P., Nathan, G. J. & Wong, C. Y. 2007 PIV measurements of a turbulent jet issuing from round sharp-edged plate. *Experiments in Fluids* **42** (4), 625–637. https://doi.org/10.1007/s00348-007-0271-9.

Mi, J., Feng, B., Deo, R. C. & Nathan, G. J. 2009 Effect of exit Reynolds number on self-preservation of a plane jet. *Acta Physica Sinica* **58** (11), 7756–7764.

Miller, R. S., Madnia, C. K. & Givi, P. 1995 Numerical simulation of non-circular jets. *Computers & Fluids* **24** (1), 1–25. https://doi.org/10.1016/0045-7930(94)00019-U.

Moeini, M., Khorsandi, B. & Mydlarski, L. 2020 Effect of acoustic Doppler velocimetry sampling frequency on statistical measurements of turbulent axisymmetric jets. *Journal of Hydraulic Engineering* **146** (7), 4020048. https://doi.org/10.1061/(ASCE)HY.1943-7900.0001767.

Moeini, M., Khorsandi, B. & Mydlarski, L. 2021 Effect of coflow turbulence on the dynamics and mixing of a non-buoyant turbulent jet. *Journal of Hydraulic Engineering* **147** (1), 04020088. https://doi.org/10.1061/(ASCE)HY.1943-7900.0001830.

Nikora, V. I. & Goring, D. G. 1998 ADV measurements of turbulence: can we improve their interpretation? *Journal of Hydraulic Engineering* **124** (6), 630–634. https://doi.org/10.1061/(ASCE)0733-9429(2002)128:1(117).

Panchapakesan, N. R. & Lumley, J. L. 1993 Turbulence measurements in axisymmetric jets of air and helium. Part 1. Air jet. *Journal of Fluid Mechanics* **246**, 197–223. https://doi.org/10.1017/S0022112093000096.

Pope, S. B. 2000 *Turbulent Flows*. IOP Publishing.

Quinn, W. R. 1989 On mixing in an elliptic turbulent free jet. *Physics of Fluids A: Fluid Dynamics* **1** (10), 1716–1722. https://doi.org/10.1063/1.857536.

Quinn, W. R. 1991 Passive near-field mixing enhancement in rectangular jet flows. *AIAA Journal* **29** (4), 515–519. https://doi.org/10.2514/3.10613.

Quinn, W. R. 2005 Measurements in the near flow field of an isosceles triangular turbulent free jet. *Experiments in Fluids* **39** (1), 111–126. https://doi.org/10.1007/s00348-005-0988-2.

Quinn, W. R., Azad, M. & Groulx, D. 2013 Mean streamwise centerline velocity decay and entrainment in triangular and circular jets. *AIAA Journal. American Institute of Aeronautics and Astronautics* **51** (1), 70–79. https://doi.org/10.2514/6.2011-3087.

Ricou, F. P. & Spalding, D. B. 1961 Measurements of entrainment by axisymmetrical turbulent jets. *Journal of Fluid Mechanics* **11** (1), 21–32. https://doi.org/10.1017/S0022112061000834.

Schlichting, V. H. 1933 Laminare strahlausbreitung. *ZAMM-Journal of Applied Mathematics and Mechanics/Zeitschrift für Angewandte Mathematik und Mechanik* **13** (4), 260–263.

Trüpel, A. W. T. 1914 *Über die Einwirkung Eines Luftstrahles auf die Umgebende Luft*. Oldenbourg, Germany.

Wahl, T. L. 2003 Discussion of 'Despiking acoustic doppler velocimeter data" by Derek G. Goring and Vladimir I. Nikora. *Journal of Hydraulic Engineering* **129** (6), 484–487.

Wygnanski, I. & Fiedler, H. 1969 Some measurements in the self-preserving jet. *Journal of Fluid Mechanics* **38** (3), 577–612. https://doi.org/10.1017/S0022112069000358.

Xu, G. & Antonia, R. 2002 Effect of different initial conditions on a turbulent round free jet'. *Experiments in Fluids* **33** (5), 677–683. https://doi.org/10.1007/s00348-002-0523-7.

Xu, M., Pollard, A., Mi, J., Secretain, F. & Sadeghi, H. 2013a Effects of Reynolds number on some properties of a turbulent jet from a long square pipe. *Physics of Fluids* **25** (3), 35102. https://doi.org/10.1063/1.4797456.

Xu, M., Zhang, J., Mi, J., Nathan, G. J. & Kalt, P. A. M. 2013b PIV measurements of turbulent jets issuing from triangular and circular orifice plates. *Science China Physics, Mechanics and Astronomy* **56** (6), 1176–1186. https://doi.org/10.1007/s11433-013-5099-0.

First received 23 August 2021; accepted in revised form 27 October 2021. Available online 5 November 2021

Downloaded from http://iwaponline.com/wst/article-pdf/84/12/3907/980074/wst084123907.pdf
by guest